Light Metals 2012 *Edited by: Carlos E. Suarez*
TMS (The Minerals, Metals & Materials Society), 2012

Impact of Amperage Creep on Potroom Busbars: Thermal-Mechanical Aspects

Andre Felipe Schneider, Daniel Richard and Olivier Charette

Hatch, 5 Place Ville-Marie, Suite 200, Montréal, Québec, Canada, H3B 2G2

Keywords: Amperage Creep, DC Busbars, Finite Element Analysis, Thermal-Mechanical Modeling

Abstract

The mechanical performance of pot-to-pot busbars is intimately linked to the temperature and thermal expansion of conductors. With amperage creep, busbars are typically running hotter than they were at start-up, so that adequate temperature fields for both standard and bypass conditions must be considered to accurately represent the thermal stresses acting over the system.

To assist smelters to evaluate the performances of busbars systems under realistic operating conditions, a methodology was developed using ANSYS™-based numerical simulation, where the temperature field obtained from a thermal-electrical model is applied as a load to a thermal-mechanical model. The bolted connections at the shunting-clamping stations, the weld plates and the contact mechanics between bars are taken into account explicitly.

A test case based on a demonstration busbar system is presented and the typical impact of line current and selected operational procedures on thermal-mechanical performance and reliability of specific design features is discussed.

Introduction

Busbars are an integral part of the aluminium reduction technology and their design has a profound impact on the stability and performance of cells, notably through magneto-hydro-dynamics (MHD) effects. However, on the most basic level, their purpose is to collect current from the cathodic part of a cell and feed it to the anodic part of the next. Busbars are also needed to connect groups of cells, for example at passageways and between potrooms, and to carry the electrical current to and from the rectifiers.

The reliable operation of these conductors and their insulating materials is therefore of capital importance to sustaining smelter operations and workers safety. Past experience has shown that the window for a trouble-free operation of these components tends to reduce with increasing ambient temperature, pot line current and contact resistance between non-welded assemblies, such as in bolted connections and short-circuiting stations.

The mechanical performance of pot-to-pot busbars is intimately linked to the temperature and thermal expansion of conductors. With amperage creep, busbars are typically running hotter than they were at start-up, so that adequate temperature fields for both standard and bypass conditions must be considered to accurately represent the thermal stresses acting over the system.

Pot-to-pot Busbars Thermal-Mechanical Behavior

The thermal-mechanical (TM) behavior of structures is a complex, displacement-controlled problem. If a given body is submitted to a condition that differs from its expansion-free temperature, it will experience a change on its dimensions – the linear thermal expansion can be calculated by Equation (1).

$$\Delta L = L_0 \cdot \chi_{th}\left(T_{Eqv} - T_0\right) \qquad (1)$$

Where: ΔL is the thermal expansion, [m]; L_0 is the body length measured at a reference temperature, [m]; χ_{th} is the temperature-dependant material's thermal expansion coefficient, [°C^{-1}]; T_{Eqv} is the equivalent body temperature, [°C]; and T_0 is the reference temperature, [°C]. T_0=20°C is assumed in this work.

If said component has its volume change restrained somehow, thermal-mechanical stresses will develop, typically due to the differential expansion between two different bodies (or even regions within the same body). This phenomenon is easily recognizable on the bimetallic stripe problem, Figure 1, where two different materials (with different thermal expansion coefficients $\chi_{th.1}$ and $\chi_{th.2}$) tend to develop bending stresses if they're attached together and, consequently, mutually restraining themselves.

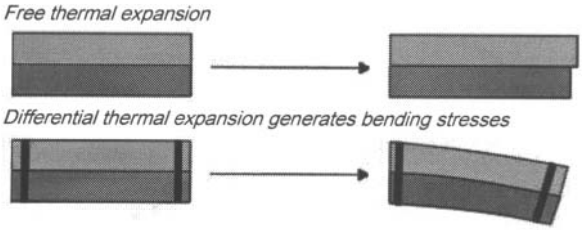

Figure 1 – Bimetallic strip problem: free vs. differential thermal expansion.

Note that the TM performance of pot-to-pot busbars is intimately linked to their temperature distribution, geometry, and interaction with conductors from neighbor cells:

- The temperature field of pot-to-pot busbars depends on ambient and pot shell temperatures, potline current, operation mode (normal operation, single or multiple bypasses) and specific operational procedures such as using or not the equalizer wedges. Thus, the resulting thermal expansion of said conductors is also to be influenced by these parameters;
- The pot-to-pot busbars system geometry may inherently lead to differential thermal expansion between its components depending on how the conductors are assembled: two parallel busbars with different temperature distributions (thus, different thermal expansions) may be welded together at two different locations which would, in turn, lead to the bimetallic stripe problem – see Figure 1;
- The cathodic busbars from a given pot are usually connected to those of its neighbors by means of tie-rods at the shunting-

clamping stations, *i.e.*, their mechanical behavior depends on the interaction between the different pot-to-pot circuits.

The calculation of the displacement and consequent stress and strain fields of pot-to-pot busbar systems is a complex, non-linear problem. In order to assist smelters to evaluate the performances of busbars systems under realistic operating conditions, a three-dimensional (3D) approach using ANSYS™-based numerical simulation was developed.

Thermal-Mechanical Pot-to-pot Busbars Model Description

In addition to providing the driving force for thermal expansion, the temperature field generated by a previously published thermal-electrical (TE) model [1] allows the evaluation of temperature-dependent aluminum properties [2, 3], shown in Figure 2 and Figure 3. The Poisson's ratio ($\nu_{xy,Al}$=0.33), the aluminum-to-aluminum friction coefficient ($\mu_{Al\text{-}Al}$=0.4) and density (ρ_{Al}=2710 kg/m^3) for the aluminum busbars are assumed to be equal to the values obtained for the alloy 1100-O [3].

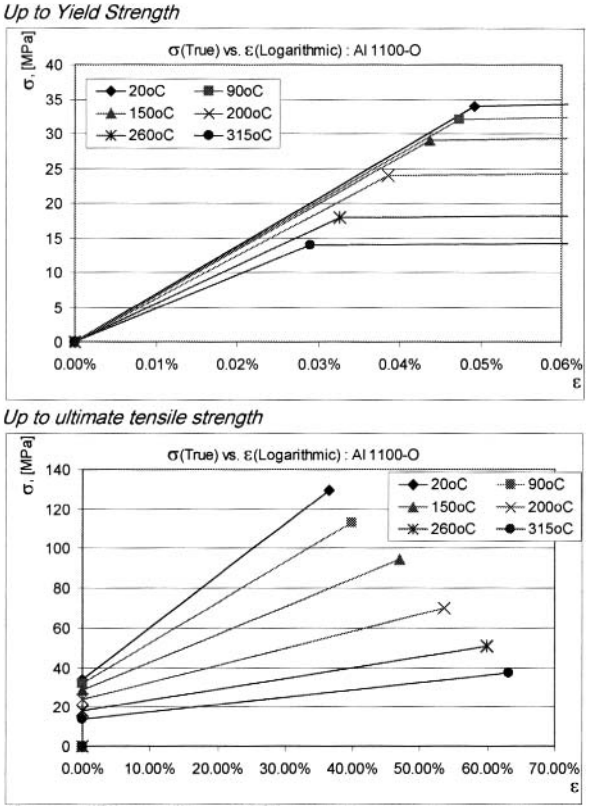

Figure 2 – Evolution of the bilinear approximation of aluminum's true stress vs. logarithmic strain curve with temperature.

All steel components are assumed to behave as low-carbon steel. The physical and mechanical properties of electrical insulators depend on the selected materials and typically vary from one technology to the other.

Alloy 1100-O

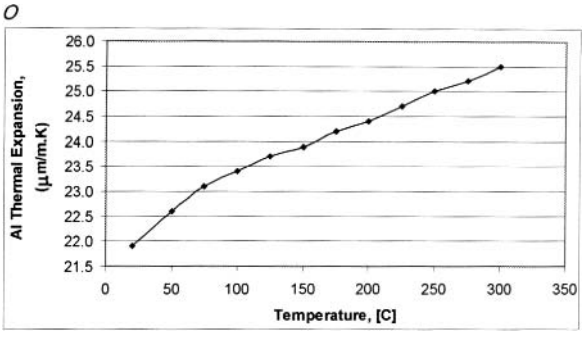

Figure 3 – Evolution of aluminum's thermal expansion coefficient with temperature.

Global TM Model

The aluminum's constitutive model considered on this global analysis, although non-linear, – see Figure 2 – is conservative[1]. The main objective of the global TM model is to evaluate the system's overall displacements and provide boundary conditions (BC) to specialized submodels, such that specific design features (like flexibles and weld plates) can be studied in greater depth. These details are simplified on the present step, being represented by solid conductors in order to take their mass into account.

To adequately represent the inherent interaction between neighbor pot-to-pot busbar systems, two typical circuit halves[2] should be connected to the full circuit of the cell of interest by means of bolted connections at both its upstream (US) and downstream (DS) shunting-clamping stations (see Figure 4):

- The spacing between the parallel busbars is dictated by the presence of steel spacer/insulator assemblies;
- The torque applied to the bolts is taken into account by a prescribed initial strain, calculated by using the Hooke's Law and torque-force relationships found in the literature [4]. Axial rotations are blocked;
- The insulating tubes encapsulating the tie-rods are modeled by means of compression-only (with gap) truss elements;
- Frictional contact-target element pairs allow for the washer/insulator-to-busbar and spacer/insulator-to-busbar mechanical interactions;
- The continuity of displacements between the two typical halves interfaces is obtained by means of coupling suitable degrees of freedom (DOF).

The reactions of the anode bridge/superstructure assembly are simulated by the usage of weak elastic foundations. Elastic foundations are also used to vertically support the conductors when the busbars-to-concrete support/insulator assembly friction coefficient $\mu_{Al\text{-}Sup}$ is considered as negligible – which in turn would cause the maximum transversal *UY* (along the potrow length) displacements, *i.e.*, a worst-case condition regarding expansion joints design. On the other hand, if $\mu_{Al\text{-}Sup}$ is not to be ignored, frictional contact-target pairs are used instead.

[1] Unloading occurs along the same path that as loading (path-independent).

[2] A typical downstream (DS) half circuit at the upstream (US) of the considered cell and a typical US half circuit at its DS.

Considered body forces (BF) include gravity and, evidently, busbars temperatures. Finally, the longitudinal *UY* displacement of the typical DS half is blocked as well as longitudinal *UX* displacement of one of its nodes.

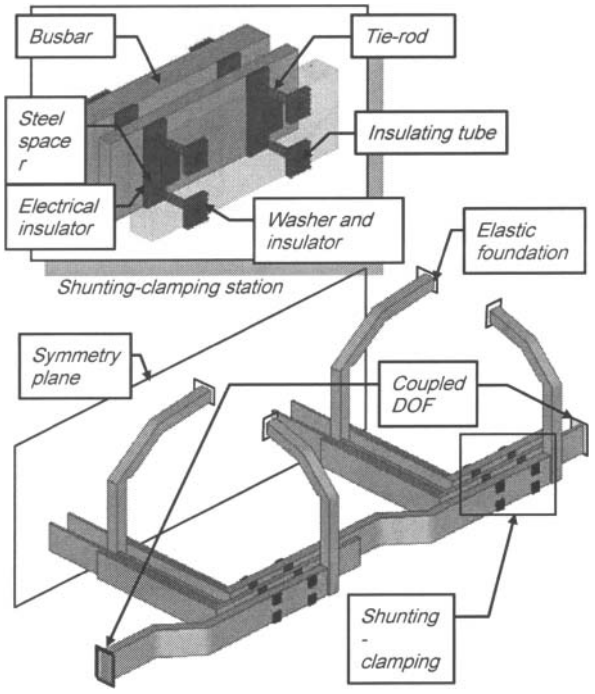

Figure 4 – TM global model.

TE and Global TM Models Relationship

The considered geometry for the global TM model is fixed and always includes all of the previously described components, as per Figure 4. On the other hand, the thermal field to be applied as body force depends on the considered operational condition, as depicted in Figure 5.

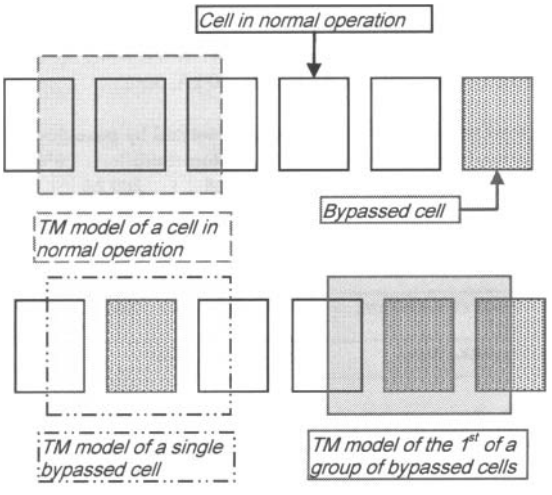

Figure 5 – Relationship between TE and global TM models.

Since both TE and TM models do *not* share the same Finite Element mesh, the relevant temperature distributions have to be interpolated from previously performed TE analyses. They're subsequently applied as prescribed DOF and the temperature diffusion problem is solved for the entire domain. The resulting thermal field is finally applied as BF for the global TM model.

Specialized Submodels

Specific design features, such as weld plates and flexible joints, can de studied in greater depth by the usage of specialized submodels. The relationship between the geometries of both global TM model and a weld plate joint submodel can be seen in Figure 6.

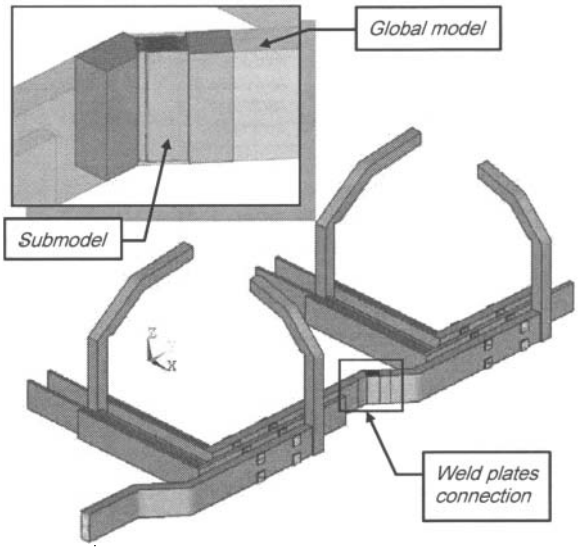

Figure 6 – Relationship between global TM model and specialized weld plate joint submodel geometries.

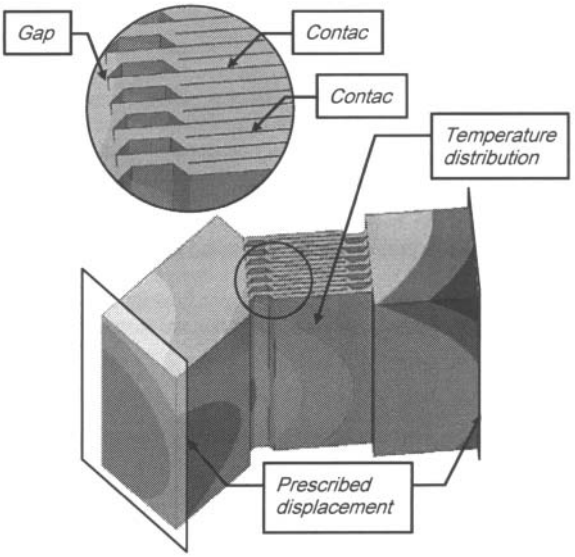

Figure 7 – Specialized weld plate joint submodel details.

The material constitutive law considers temperature-dependant kinematic linear hardening elastoplasticity and is defined using the stress-strain curves shown in Figure 2.

The displacements at the specialized submodel boundaries are interpolated directly from the global TM model displacement fields. Frictional contact-target element pairs are considered between each and every plate (or flexible sheet) of the joint, as seen in Figure 7. Finally, gravity is also taken into account.

Typical Analysis Workflow

Figure 8 shows the typical analyses[3] involved on the assessment of the pot-to-pot busbars performance.

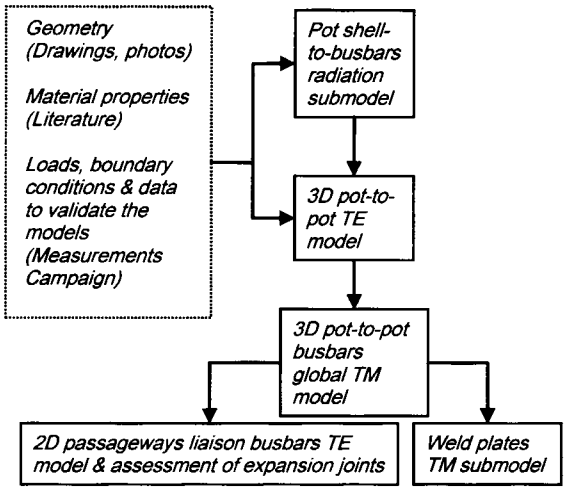

Figure 8 – Typical workflow for the assessment of the pot-to-pot busbars performance.

Test Case Model

In order to illustrate the proposed approach's capabilities, a fictitious pot-to-pot busbars circuit, previously introduced in [1], will have its TM performance assessed when running under different amperage and operational conditions[4]. Note that due symmetry reasons, only a half model will be considered.

Each pot row section in our fictitious smelter comprises 25 cells and the connection between neighbor sections is provided by passageway liaison busbars. Each one of said liaison conductors – see Figure 9 – has a flexible joint with a design capacity of 200 mm. Furthermore, note that the pot-to-pot busbars do *not* have flexible joints to accommodate their own thermal expansion.

[3] TE modeling details are provided in [1].

[4] All TE results used in this work can be found in [1].

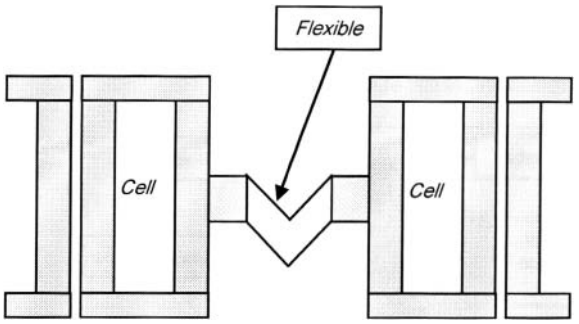

Figure 9 – Passageway liaison busbars and flexible joints.

Global TM Performance of Pot-to-pot Busbars

Figure 10 shows the predicted longitudinal *UX* and transversal *UY* busbar displacements when running the cells under normal operation conditions at 150 kA, 30°C.

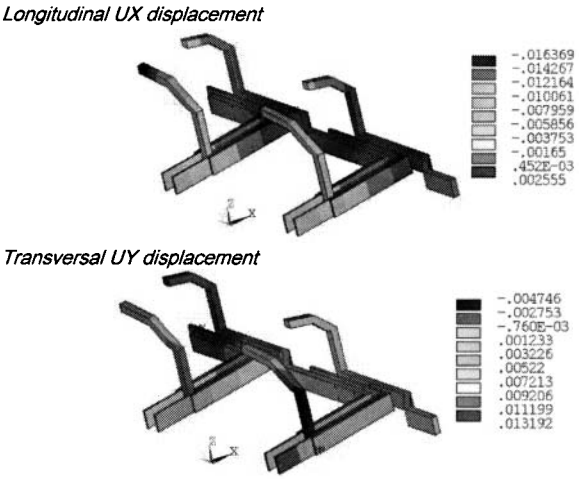

Figure 10 – Pot-to-pot busbars horizontal displacements, [m], under normal operation conditions at 150 kA, 30°C.

Table 1 shows the total expansion to be absorbed by the flexible joints from the passageway liaison busbars when running the cells under normal conditions at 150 kA and 200 kA, 30°C.

Table 1 – Total expansion joint to be absorbed by passageway expansion joints under normal operation conditions, 30°C.

	150 kA	*200 kA*
UY/cell, [mm]	*6.0*	*9.2*
# cells/pot row section, [-]	*25*	
UY/pot row section, [mm]	*150.0*	*230.0*
UY, max, [mm]	*200.0*	

Note that the expected increase in the pot-to-pot busbars transversal *UY* displacement (~ 53%) with the increasing current leads the flexible joints to be compressed beyond their design capacity. It's worth mentioning that Hatch's past experience shows that the stresses intensity on the flexible sheets wad-to-

busbar welds increases rapidly once the joints are compressed beyond their design capacity, ultimately leading to short-term damage. Figure 11 shows a real-life flexible joint that have undergone severe plastic deformation under similar conditions.

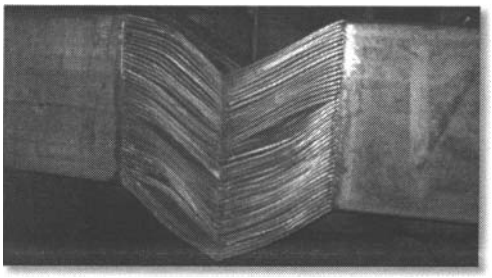

Figure 11 – Example of a buckled flexible joint.

TM Performance of Weld Plates Connections

The inner and the outer head busbar segments of our fictitious technology are connected by means of weld plates, as per Figure 6. Note that, due to their location[5], the temperatures of said connections vary drastically when passing from normal operation to bypass condition (Table 2).

Table 2 – Weld plates temperatures, [°C], under different conditions at 30°C.

	Normal Operation		*Single Bypass*	
	150 kA	*200 kA*	*150 kA*	*200 kA*
Min	*67.6*	*85.7*	*130.5*	*196.1*
Max	*68.7*	*86.4*	*138.8*	*206*

Even though no issues were found when operating the cells normally[6], stress concentrations can be seen at the busbar-to-plates welds at bypass conditions. Figure 12 and Figure 13 show, respectively, the safety factor regarding yield SF_Y distributions obtained for the connections when bypassing one cell at 150 kA and 200 kA, 30°C.

The impact of the temperature increase in the thermal-mechanical stresses acting on the weld plate joints is remarkable: the minimum safety factor regarding yield $SF_{Y,min}$ drops from 3.34 to 1.37 when increasing the current from 150 kA to 200 kA. Note that even though the welds are presently within the elastic regime, further potline current increases may lead the connections to short-term damage. A real-life example of a permanently deformed weld plates connection can be seen in Figure 14.

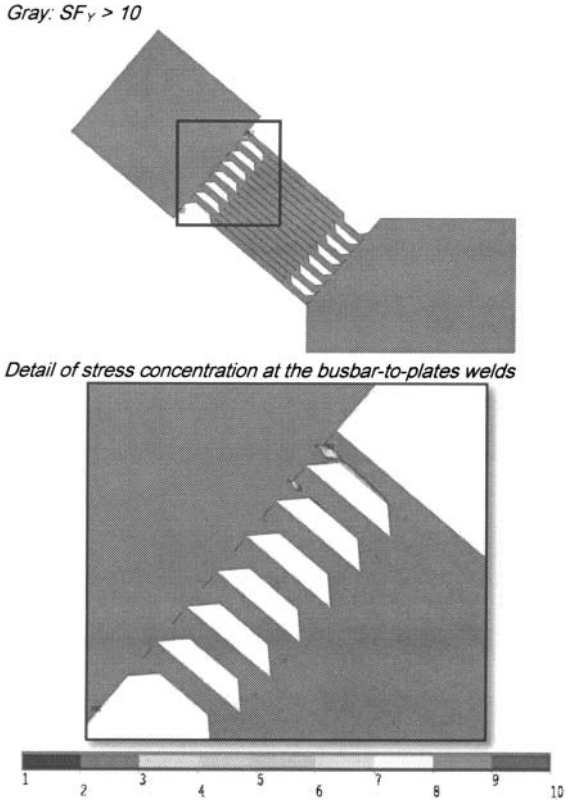

Figure 12 – Weld plates SF_Y distribution, [-], during single bypass condition at 150 kA, 30°C.

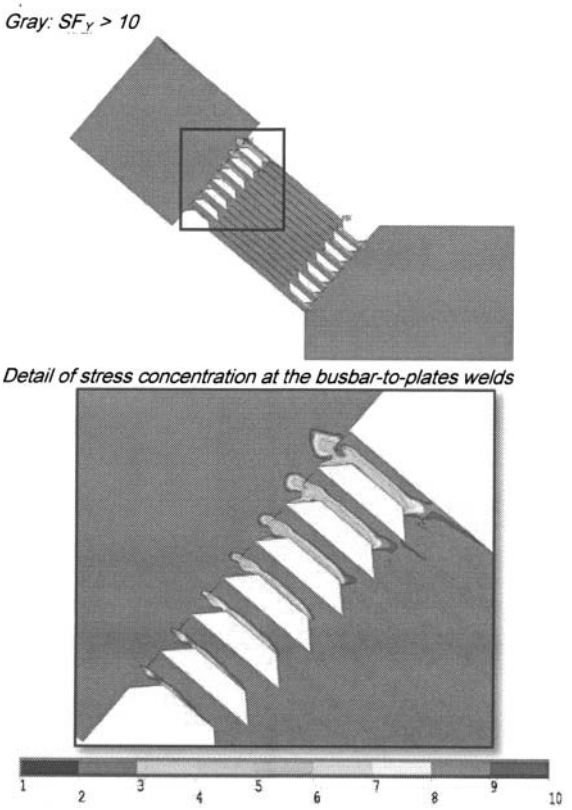

Figure 13 – Weld plates SF_Y distribution, [-], during single bypass condition at 200 kA, 30°C.

[5] Each head busbar carries ~ 25% of total potline current during normal operation and ~ 50% on bypass mode.

[6] $SF_Y > 6.6$ at 200 kA, 30°C, at normal operation conditions.

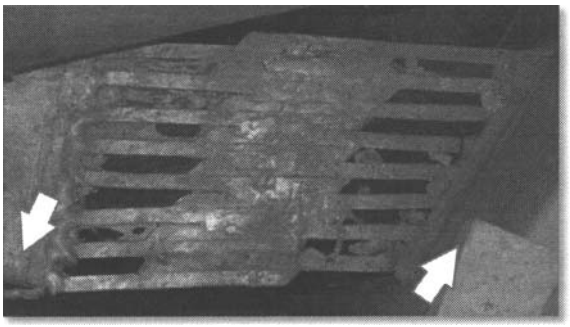

Figure 14 – Example of a permanently bent weld plates connection.

Furthermore, the roots of the welds shown in Figure 13 are mainly subjected to tensile stresses, as per Figure 15. Note that further amperage creep may lead the weld plates to develop long-term cracking due to a combined tensile creep-fatigue mechanism. In order to illustrate the real-life implications of this, a cracked weld plate is shown in Figure 16.

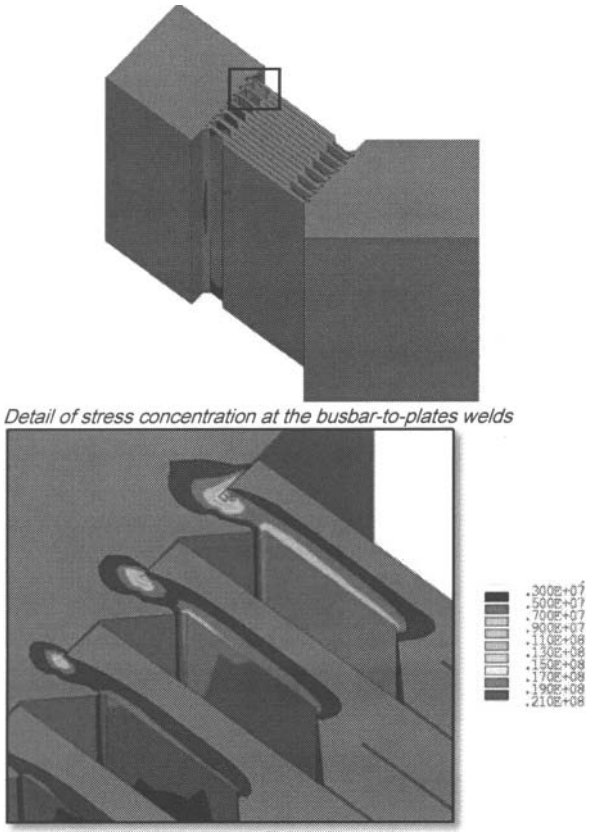

Figure 15 – 1st principal stress σ_1, [Pa], during single bypass condition at 200 kA, 30°C.

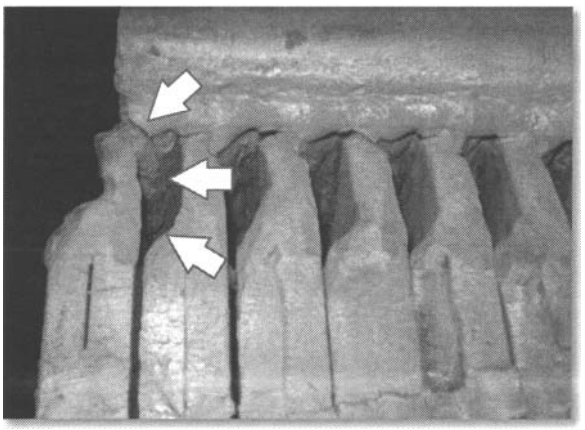

Figure 16 – Example of a cracked weld.

Conclusions

A methodology based on numerical simulation was presented for the assessment of the thermal-mechanical performance of busbars systems. It was shown that busbar design, amperage creep and operational procedures have important effects on the reliability of these systems. Furthermore, it was shown that special attention should be given to the components (weld plates and flexibles) connecting different busbars and pot row sections. Finally, evidence has shown that busbars systems should not be ignored when planning amperage creep.

References

[1] A.F. Schneider, D. Richard and O. Charette, "Impact of Amperage Creep on Busbars and Electrical Insulation: Thermal-Electrical Aspects", Proc. Light Metals 2011, TMS, Warrendale, PA, pp 525-530.

[2] J.G. Kaufman, "Aluminum Alloy Database", Knovel, 2004, Tables 4b and 10b.

[3] Boiler and Pressure Vessel Code – Section II – Part D – Subpart 2 – Physical Properties Tables, ASME, New York, 2004, pp. 672. Table TE-2.

[4] J. Shigley, "Mechanical Engineering Design", 7th Ed. McGraw-Hill, New York, 2004, pp. 1030. Eq. (8-5) and Table (8-5).